Electronic Supplementary Material (ESI) for RSC Advances.
This journal is © The Royal Society of Chemistry 2024

Supplementary Materials for

Degree of Disorder Regulated Ion Transport through Amorphous Monolayer Carbon

Shizhuo Liu[1#], Ran Cao[2#], Jiani Hu[3#], Huifeng Tian[1], Yinhang Ma[4], Honglei Xue[2], Zhenjiang Li[1], Zhixin Yao[1,5], Ruijie Li[1], PeiChi Liao[1], Yihan Wang[1], Lina Yang Zhang[1], Ge Yin[1], U Sasaki[1], Junjie Guo[5], Lifen Wang[6,7], Xiaoyan Zhang[8], Wu Zhou[4], Ji Chen[3,9], Wangyang Fu[2,9]*, and Lei Liu[1,9]*

[1] School of Materials Science and Engineering, Peking University, Beijing 100871, China

[2] School of Materials Science and Engineering, Tsinghua University, Beijing 100084, China

[3] School of Physics, Peking University, Beijing 100871, China

[4] School of Physical Sciences and CAS Key Laboratory of Vacuum Physics, University of Chinese Academy of Sciences, Beijing 100190, China

[5] Key Laboratory of Interface Science and Engineering in Advanced Materials, Ministry of Education, Taiyuan University of Technology, Taiyuan 030024, China

[6] Beijing National Laboratory for Condensed Matter Physics, Institute of Physics, Chinese Academy of Sciences, Beijing 100190, China

[7] Songshan Lake Materials Laboratory, Dongguan, Guangdong 523808, China

[8] School of Pharmaceutical Sciences, Capita Medical University, Beijing 100069, China

[9] Interdisciplinary Institute of Light-Element Quantum Materials and Research Center for Light-Element Advanced Materials, Peking University, Beijing 100871, China

# These authors contributed equally to this work

* Correspondence: fwy2018@mail.tsinghua.edu.cn; l_liu@pku.edu.cn;

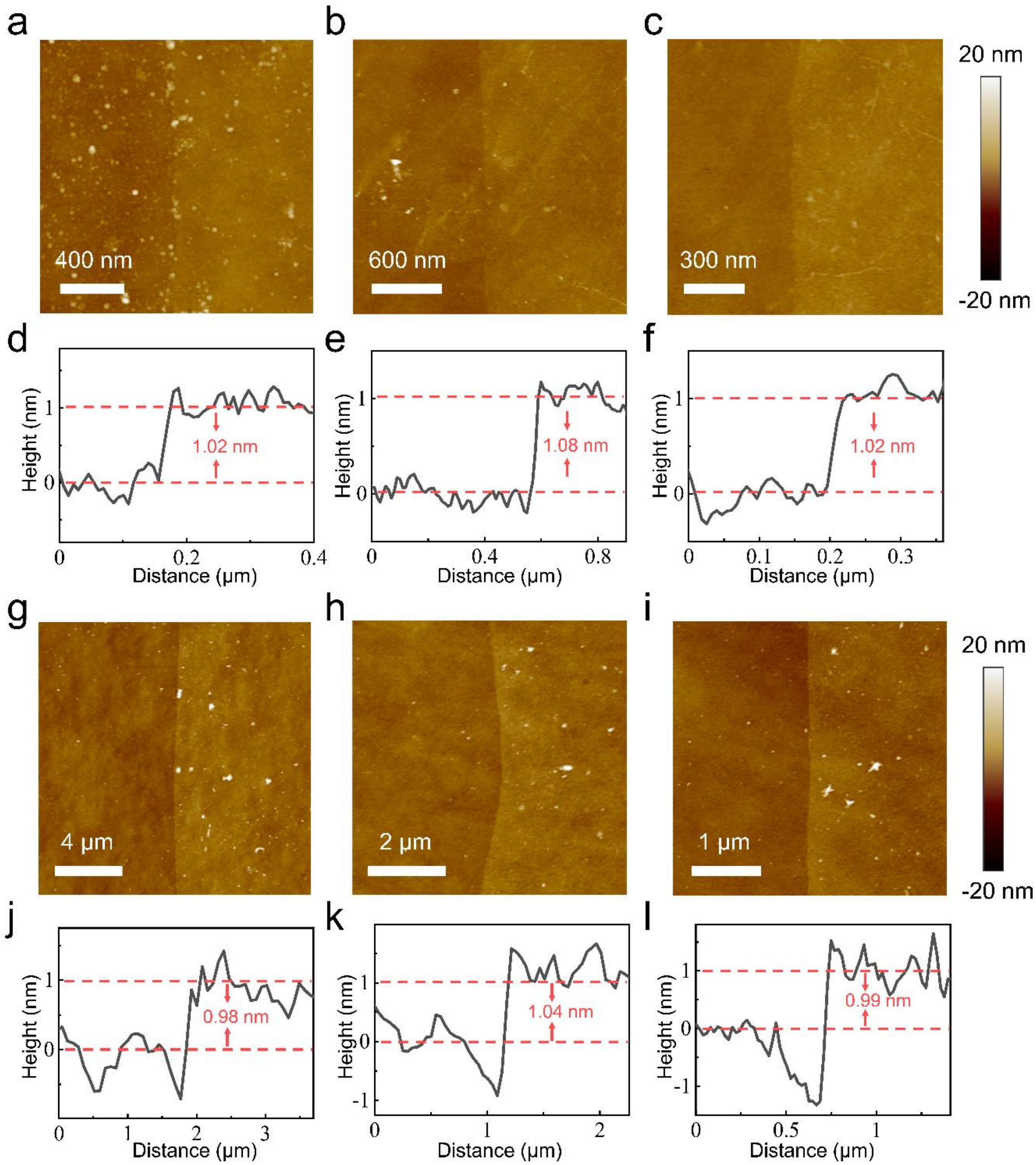

Supplementary Figure 1. AFM characterizations of AMC-400 (1a-1f) and AMC-600 (1g-1l), respectively, after transferring onto SiO_2/Si substrates, showing a uniform thickness of ~ 1 nm.

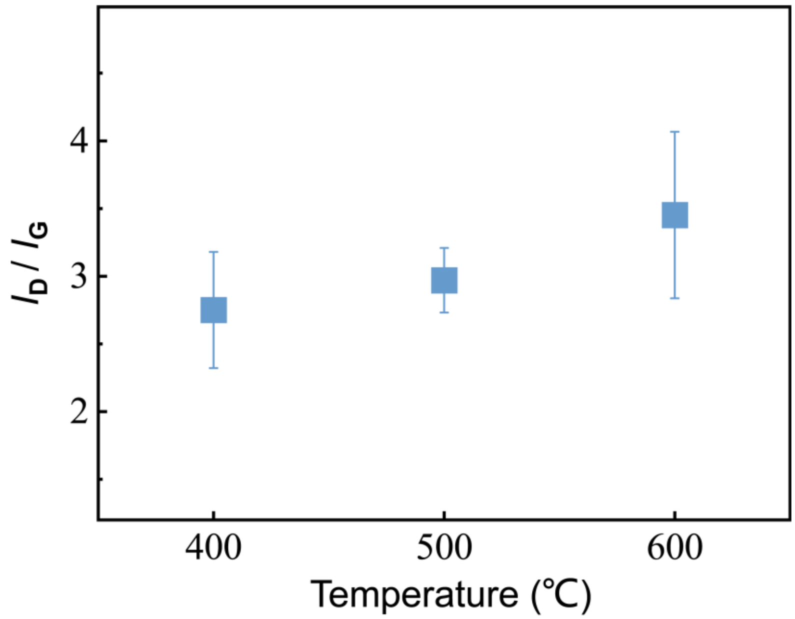

Supplementary Figure 2. I_D/I_G (area ratio) versus the synthesis temperatures for AMC samples. After analyzing multi-Raman spectra (> 50), I_D/I_G slightly increases with the synthesis temperature, but with a large variation and uncertainty for each data point.

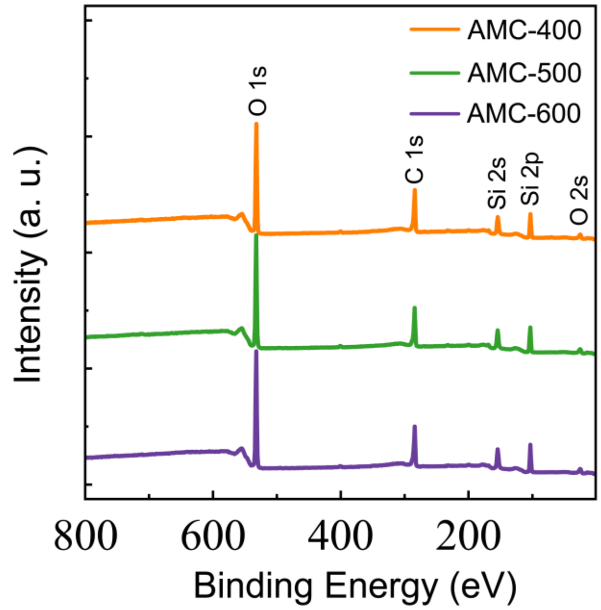

Supplementary Figure 3. Full scan of XPS on AMC-400, AMC-500, and AMC-600, respectively, after transferring onto SiO_2/Si substrates.

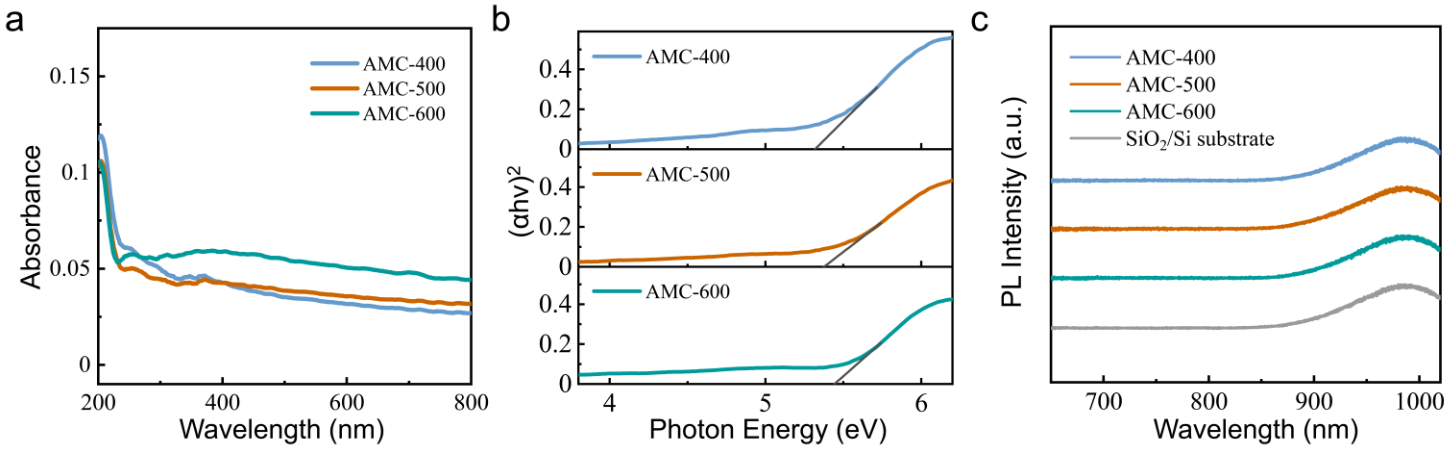

Supplementary Figure 4. More spectroscopic characterizations on AMC samples. (a, b) UV-Vis absorbance spectra and derived optical bandgaps of 5.32 eV, 5.38 eV, and 5.44 eV, corresponding to AMC-300, AMC-400, and AMC-500 respectively. (c) Photoluminescence spectra of AMC samples. The excitation wavelength is 532 nm.

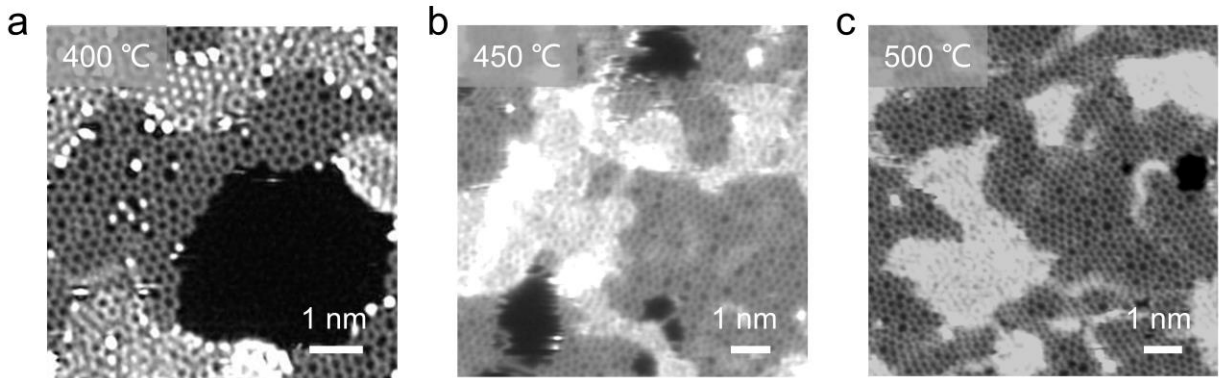

Supplementary Figure 5. Additional STEM images to show the relatively large nanopores for AMC-400 (a), AMC-450 (b), and AMC-500 (c), respectively.

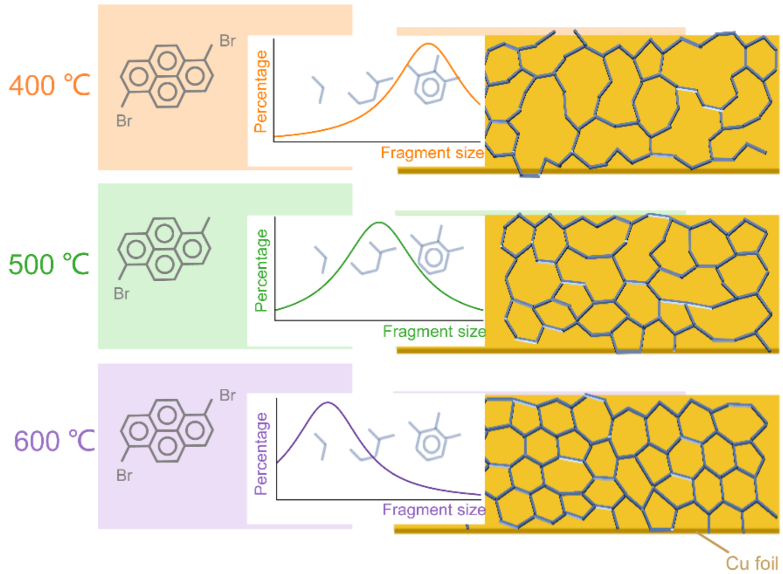

Supplementary Figure 6. Schematic diagram of AMC growth process under varying temperatures. When the precursor is exposed to different temperatures, distinct crack levels can result in different distribution of fragments. For example, at higher temperature the molecules experience more thorough thermal cracking. This feature, combined with the temperature-tuned catalytic property of Cu surface and species mobility, together determine the different level of nanopores, in terms of the size and density, in the as-grown AMC films.

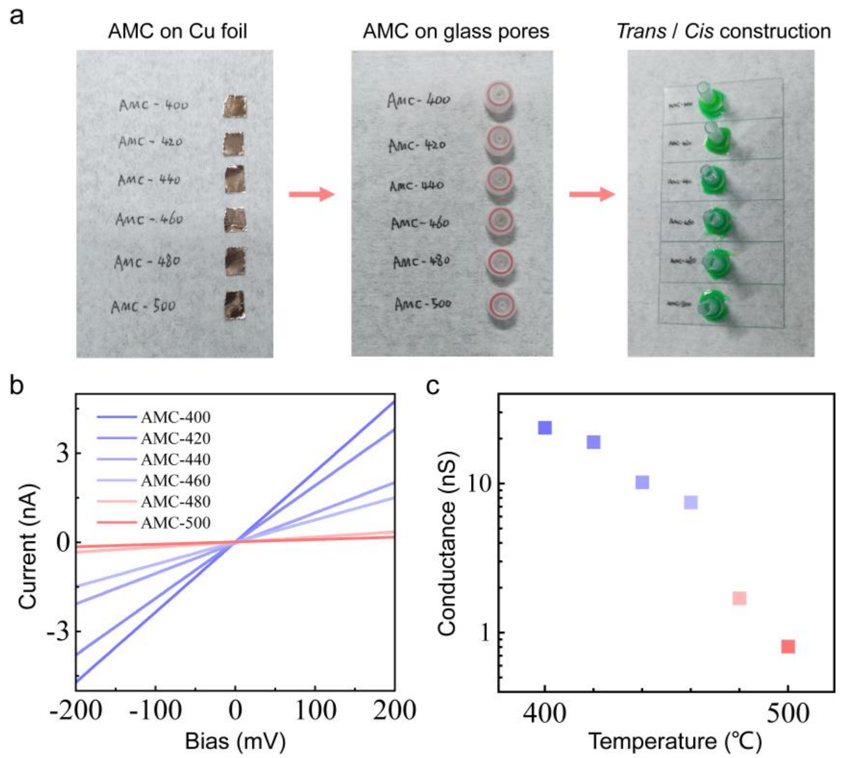

Supplementary Figure 7. More transmembrane ionic transport measurements of AMC samples obtained between 400 °C and 500 °C. (a) Optical image of AMC samples on Cu foils (left column), after transferring onto glass pores (middle column), and on the *Trans*/*Cis* chips. (b) The transmembrane current versus bias curves. (c) The transmembrane conductance of AMC samples calculated from *I-V* curves in (b).

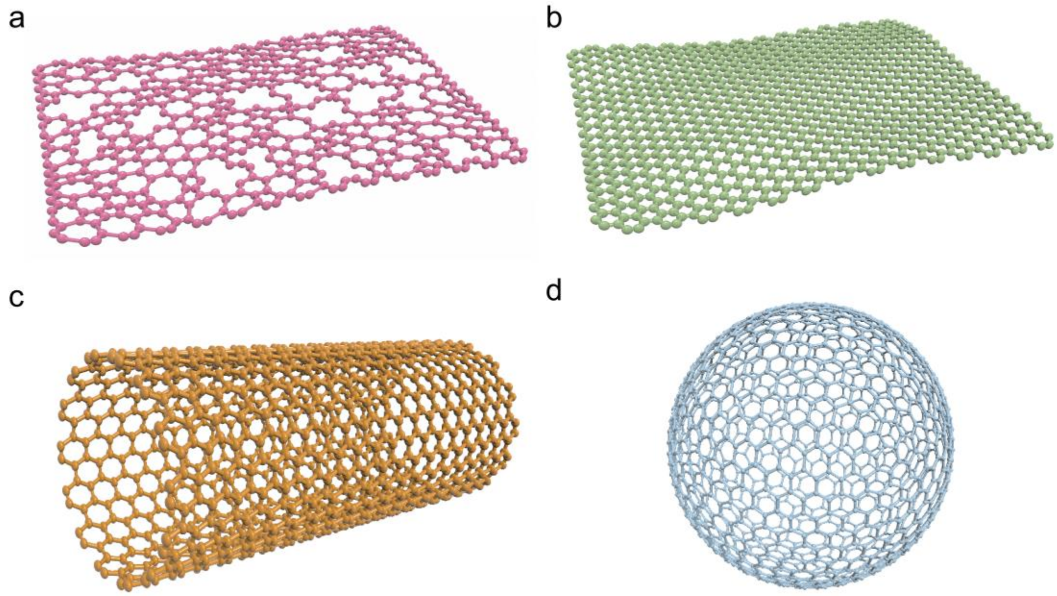

Supplementary Figure 8. Schematic diagram of carbon nanomaterials: AMC (a), graphene (b), carbon nanotube (c), and fullerene (d).

Supplementary Table 1. Comparison of AMC with other 2D materials reported as ionic transmembrane.

Materials	Nanopore Fabrication	Pore Size	Testing Area	Conductance
Graphene [1-4]	Electron irradiation	5-23 nm	0.04 μm^2	50-240 nS
	Electrochemical reaction	-	0.8 μm^2	0.4-16 nS
	O_2 plasma treatment	-	0.2 mm^2	0.14-11 nS
	Ga^+/He^+ ion bombardment or H_2/N_2 plasma treatment	0.4-3 nm	20 μm^2	2-8 nS (0.1 M KCl)
MoS_2 [5-7]	Electron irradiation or electrochemical reaction	2-25 nm	3-500 nm^2	20-300 nS
	Ga^+ ion bombardment	0.4-1.4 nm	0.03 μm^2	0.02-3 nS
	PAN etchant reaction	14-26 nm	0.008 μm^2	0.9-130 nS
WS_2 [8]	Electron irradiation	2-8 nm	0.07 μm^2	27-108 nS
AMC (This work)	None	0-4 nm	0.8 μm^2	0.6-23 nS

References:

1. S. Garaj, W. Hubbard, A. Reina, J. Kong, D. Branton and J. A. Golovchenko, *Nature*, 2010, **467**, 190-193.
2. X. Zhang, P. M. G. van Deursen, W. Fu and G. F. Schneider, *ACS Sens.*, 2020, **5**, 2317-2325.
3. A. K. Niketa and S. Kumar, *ACS Appl. Mater. Interfaces*, 2024, **16**, 5294-5301.
4. P. Chaturvedi, I. V. Vlassiouk, D. A. Cullen, A. J. Rondinone, N. V. Lavrik and S. N. Smirnov, *ACS Nano*, 2019, **13**, 12109-12119.
5. J. Feng, M. Graf, K. Liu, D. Ovchinnikov, D. Dumcenco, M. Heiranian, V. Nandigana, N. R. Aluru, A. Kis and A. Radenovic, *Nature*, 2016, **536**, 197-200.
6. J. P. Thiruraman, K. Fujisawa, G. Danda, P. M. Das, T. Y. Zhang, A. Bolotsky, N. Perea-López, A. Nicolaï, P. Senet, M. Terrones and M. Drndic, *Nano Lett.*, 2018, **18**, 1651-1659.
7. P. M. Das, J. P. Thiruraman, Y. C. Chou, G. Danda and M. Drndic, *Nano Lett.*, 2019, **19**, 392-399.
8. G. Danda, P. M. Das, Y. C. Chou, J. T. Mlack, W. M. Parkin, C. H. Naylor, K. Fujisawa, T. Y. Zhang, L. B. Fulton, M. Terrones, A. T. C. Johnson and M. Drndic, *ACS Nano*, 2017, **11**, 1937-1945.